

CONTROL OF SIDESLIP AND YAW RATE IN 4-WHEEL STEERING CARS USING PARTIAL DECOUPLING AND INDIVIDUAL CHANNEL DESIGN

M. A. Vilaplana, D. Leith, W. E. Leithead

Hamilton Institute, National University of Ireland, Maynooth, Co. Kildare, Ireland

Keywords: Vehicle dynamics and control, 4-wheel steering, partially decoupled systems, Individual Channel Design.

Abstract

This paper presents a new steering control structure for cars equipped with 4-wheel steering. This control structure is based on a simplified linear model of the lateral dynamics of such cars and aims to decouple the control of sideslip from the control of yaw rate. The control design is based on a linear multivariable plant which incorporates the model of the lateral dynamics mentioned above and whose inputs are linear combinations of the front and rear steering angles. The plant also contains a cross-feedback element. The matrix transfer function of the resulting plant is upper-triangular (partially decoupled). The MIMO design problem can then be recast as two SISO design problems using channel decomposition according to the Individual Channel Design (ICD) paradigm. The proposed control structure has been applied to design sideslip and yaw rate controllers using a more accurate model of the lateral dynamics of 4-wheel steering cars. This model incorporates the tyre force dynamics and the steering actuators. Simulations are used to illustrate the performance and robustness of the designed controllers.

1 Introduction

This paper presents a feedback control structure which aims to enable 4-wheel steering cars to accurately track given reference sideslip and yaw rate signals corresponding to the course desired by the driver. It is assumed that the output variables to be controlled, yaw rate and sideslip angle, are measured (in practice, the latter might typically be estimated using, for example, a Kalman filter). A 4-wheel steering car implementing the proposed control structure is also expected to automatically reject any disturbances in sideslip and yaw rate caused by lateral gusts of wind or μ -split braking situations. The controlled car must be robustly stable, particularly with respect to changes in tyre characteristics.

Most of the previous work on 4-wheel active steering focuses on using gain scheduled feedforward to control the rear wheels, thereby improving the manoeuvrability and cornering performance of the vehicle [2]. The work described in [3] proposes a feedback control structure based on Virtual Model Following Control and robust LQR design. The model to be followed corresponds to the front-wheel steered car. In [1], a control structure based on the cross-feedback of the yaw rate to the front steering angle is presented. This structure

decouples the control of the lateral acceleration of the front axle from the control of the yaw rate. Two outer feedback loops are used to allow the front wheels to control the lateral acceleration and enable the rear wheels to reduce the damping of the resulting yaw dynamics.

The control structure proposed in this paper is based on a simplified linear model of the lateral dynamics of 4-wheel steering cars at constant speed. This model relies on a single-track model of the car and linearised tyre stiffness. With the objective of decoupling the control of sideslip from that of yaw rate, the controlled inputs are chosen to be linear combinations of the front and rear steering angles and a cross-feedback element is introduced. The resulting plant to be controlled is upper-triangular and allows for the design of a sideslip controller and a yaw rate controller using classical SISO techniques. The proposed control structure has been used to design sideslip and yaw rate controllers considering a more accurate single-track model of 4-wheel car steering dynamics. This model includes tyre force dynamics and actuators. Simulations are used to illustrate the performance and robustness of the proposed controllers.

The remainder of this paper is structured as follows. Section 2 presents the simplified model of the lateral dynamics of a 4-wheel steering car used to define the proposed control structure. Section 3 introduces channel decomposition in multivariable plants according to the Individual Channel Design paradigm [4]. This section also shows that, in the case of partially decoupled plants with 2 inputs and 2 outputs, channel decomposition transforms the MIMO design problem into two SISO ones. Section 4 describes the proposed control structure, which relies on input transformation and cross-feedback to transform the control design problem at hand into the problem of controlling a partially decoupled plant with 2 inputs and 2 outputs. Section 5 describes how the proposed control structure can be used to design yaw rate and sideslip controllers for a more accurate model of the car lateral dynamics. Section 6 presents simulations illustrating the performance and robustness of the controllers. Finally, in Section 7 the conclusions of the work presented in this paper are stated and issues for future research are proposed.

2 Simplified linear model of the lateral dynamics of 4-wheel steering cars

Throughout this paper, it is assumed that the essential features of the car lateral dynamics can be described using the single-track model [3]. The single-track model is obtained by

lumping the two front wheels into a single wheel at the centre of the front axle and lumping the two rear wheels into a single wheel at the centre of the rear axle. It is assumed that the two front wheels are steered the same angle and so are the two rear wheels. The roll, pitch and heave motions of the car are disregarded and the motion is assumed to take place in the horizontal plane. Figure 1 depicts the single-track model indicating the main elements necessary for the analysis of the lateral dynamics.

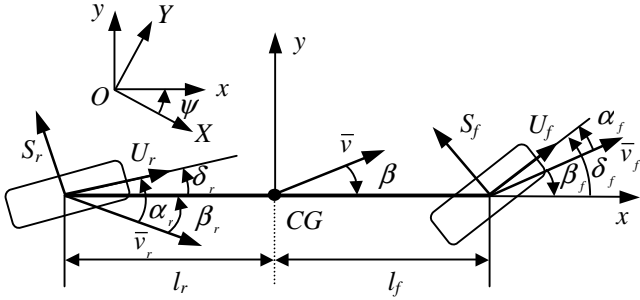


Figure 1. Single-track model of the car.

The equations of motion are applied to the single-track model and linearised about an equilibrium point characterised by constant speed and zero steering angles. The result is the following linear time-invariant system with inputs δ_f and δ_r (front and rear steering angles) and outputs β and $\dot{\psi}$ (sideslip angle and yaw rate):

$$\begin{aligned} \dot{x} &= Ax + Bu \\ y &= Cx + Du \\ u &= \begin{bmatrix} \delta_f \\ \delta_r \end{bmatrix}, \quad y = x = \begin{bmatrix} \beta \\ \dot{\psi} \end{bmatrix} \\ A &= \begin{bmatrix} -\frac{C_f + C_r}{mv_x} & \frac{C_f l_f - C_r l_r}{mv_x^2} + 1 \\ \frac{C_f l_f - C_r l_r}{I_{zz}} & -\frac{C_f l_f^2 + C_r l_r^2}{I_{zz} v_x} \end{bmatrix}, \\ B &= \begin{bmatrix} -\frac{C_f}{mv_x} & -\frac{C_r}{mv_x} \\ \frac{C_f l_f}{I_{zz}} & -\frac{C_r l_r}{I_{zz}} \end{bmatrix}, \quad C = \begin{bmatrix} 1 & 0 \\ 0 & 1 \end{bmatrix}, \quad D = \begin{bmatrix} 0 & 0 \\ 0 & 0 \end{bmatrix} \end{aligned} \quad (1)$$

The transfer function corresponding to the state-space representation above is given by:

$$G(s) = C(sI - A)^{-1} B + D = \begin{bmatrix} g_{11}(s) & g_{12}(s) \\ g_{21}(s) & g_{22}(s) \end{bmatrix} \quad (2)$$

3 Individual channel decomposition and partial decoupling

Suppose that the car lateral dynamics are to be controlled as depicted in Figure 2.

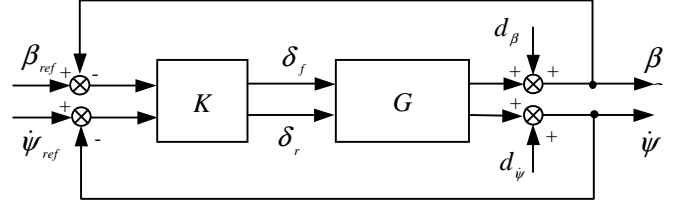


Figure 2. Generic 2 by 2 control system.

To simplify the design process, it is assumed that the 2 by 2 transfer function matrix G in Figure 2, which describes the car steering response, is the one in (2). If the controller K is assumed to be diagonal, then the multivariable control system in Figure 2 can be decomposed into two SISO control systems called channels which together are fully equivalent to the original system [4]. The two channels obtained from the decomposition are shown in Figure 3 below.

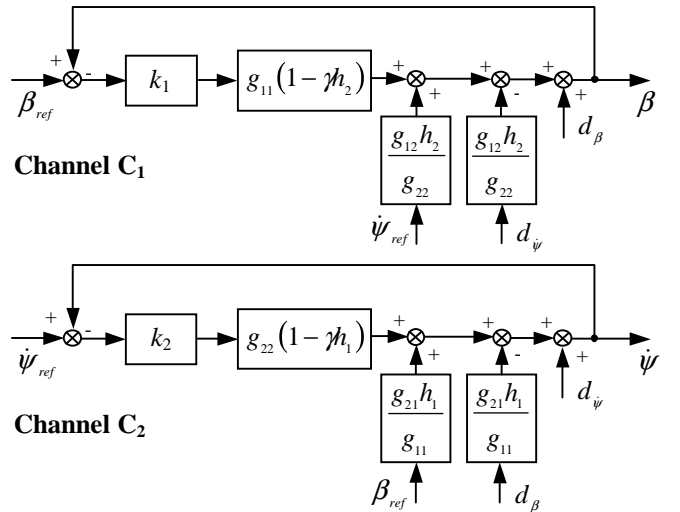


Figure 3. Individual channel decomposition.

The channel decomposition in Figure 3 is based on the following functions:

$$\begin{aligned} \gamma(s) &= \frac{g_{12}(s)g_{21}(s)}{g_{11}(s)g_{22}(s)}, \\ h_1(s) &= \frac{k_1(s)g_{11}(s)}{1 + k_1(s)g_{11}(s)}, \quad h_2(s) = \frac{k_2(s)g_{22}(s)}{1 + k_2(s)g_{22}(s)} \end{aligned} \quad (3)$$

The closed-loop response of the channels to the reference inputs β_{ref} and $\dot{\psi}_{ref}$ are given by:

$$\begin{aligned} \text{Channel 1: } \beta(s) &= t_{11}(s)\beta_{ref}(s) + t_{12}(s)\dot{\psi}_{ref}(s) \\ \text{Channel 2: } \dot{\psi}(s) &= t_{21}(s)\beta_{ref}(s) + t_{22}(s)\dot{\psi}_{ref}(s) \end{aligned} \quad (4)$$

$$t_{ii}(s) = \frac{c_i(s)}{1 + c_i(s)}, \quad i = 1, 2 \quad (5)$$

$$t_{ij}(s) = \frac{g_{ij}(s)h_j(s)}{g_{ji}(s)}(1 + c_i(s))^{-1}, \quad i = 1, 2 \quad j = 1, 2 \quad i \neq j$$

The term $c_i(s)$ in (5) is the open-loop transmittance of channel i , which is defined as

$$c_i(s) = k_i(s)g_{ii}(s)(1 - \gamma(s)h_j(s)), \quad i = 1, 2 \quad j = 1, 2 \quad i \neq j \quad (6)$$

The closed-loop response of the channels to the disturbance inputs d_β and d_ψ is as follows:

$$\begin{aligned} \text{Channel 1: } \beta(s) &= s_{11}(s)d_\beta(s) + s_{12}(s)d_\psi(s) \\ \text{Channel 2: } \dot{\psi}(s) &= s_{21}(s)d_\beta(s) + s_{22}(s)d_\psi(s) \end{aligned} \quad (7)$$

$$\begin{aligned} s_{ii}(s) &= \frac{1}{1 + c_i(s)}, \quad i = 1, 2 \\ s_{ij}(s) &= -\frac{g_{ij}(s)h_j(s)}{g_{jj}(s)}(1 + c_i(s))^{-1} = -t_{ij}, \quad i = 1, 2 \quad j = 1, 2 \quad i \neq j \end{aligned} \quad (8)$$

Robust stability of the multivariable control system is equivalent to the robust stability of the channels providing that neither of the two multivariable structure functions $\gamma(s)h_j(s)$ comes close to the (1,0) point [4].

Suppose that, instead of $G(s)$, a plant $\tilde{G}(s)$ describing the car lateral dynamics with the same outputs β and $\dot{\psi}$ but with different inputs is to be controlled. If $\tilde{G}(s)$ is upper-triangular ($\tilde{g}_{21}(s) = 0$), then $\tilde{\gamma}(s) = 0$ and the transmittances of the resulting channels are given by

$$\tilde{c}_1(s) = \tilde{k}_1(s)\tilde{g}_{11}(s), \quad \tilde{c}_2(s) = \tilde{k}_2(s)\tilde{g}_{22}(s) \quad (9)$$

In this case, the desired specifications for the controlled system can in principle be met with a $\tilde{k}_1(s)$ designed on the basis of $\tilde{g}_{11}(s)$ and a $\tilde{k}_2(s)$ designed on the basis of $\tilde{g}_{22}(s)$, with due regard to $\frac{\tilde{g}_{12}(s)\tilde{h}_2(s)}{\tilde{g}_{22}(s)}$ for cross-coupling rejection.

The influence of cross coupling on the performance of Channel 2 is negligible regardless of the controller $\tilde{k}_1(s)$ in place, since $\tilde{t}_{21}(s) = 0$ and $\tilde{s}_{21}(s) = 0$. The cross-coupling rejection performance of Channel 1 depends on $\frac{\tilde{g}_{12}(s)\tilde{h}_2(s)}{\tilde{g}_{22}(s)}$,

which may have to be taken into account in the design of $\tilde{k}_2(s)$.

4 Partial decoupling using input transformation and cross-feedback

Suppose the simplified linear dynamics of the single-track model described by (1) can also be expressed as follows:

$$\begin{aligned} \dot{x} &= \tilde{A}x + \tilde{B}\tilde{u} \\ y &= \tilde{C}x + \tilde{D}\tilde{u} \end{aligned} \quad (10)$$

where

$$\begin{aligned} \tilde{u} &= \begin{bmatrix} \Delta_1 \\ \Delta_2 \end{bmatrix} = E \begin{bmatrix} \delta_f \\ \delta_r \end{bmatrix}, \quad y = x = \begin{bmatrix} \beta \\ \dot{\psi} \end{bmatrix}, \\ \tilde{A} &= \begin{bmatrix} \tilde{a}_{11} & \tilde{a}_{12} \\ 0 & \tilde{a}_{22} \end{bmatrix}, \quad \tilde{B} = \begin{bmatrix} \tilde{b}_{11} & 0 \\ 0 & \tilde{b}_{22} \end{bmatrix}, \\ \tilde{C} &= \begin{bmatrix} 1 & 0 \\ 0 & 1 \end{bmatrix}, \quad \tilde{D} = \begin{bmatrix} 0 & 0 \\ 0 & 0 \end{bmatrix} \end{aligned} \quad (11)$$

The matrix E defines two new inputs Δ_1 and Δ_2 as linear combinations of the front and rear steering angles. According to the state-space representation above, the yaw rate is governed by the following equation:

$$\dot{\psi} = \tilde{a}_{22}\dot{\psi} + \tilde{b}_{22}\Delta_2 \quad (12)$$

This implies that $\dot{\psi}(s)$ does not depend directly on $\Delta_1(s)$ and, consequently, the transfer function corresponding to the state-space representation (10)-(11) is of the form:

$$\tilde{G}(s) = \tilde{C}(sI - \tilde{A})^{-1}\tilde{B} + \tilde{D} = \begin{bmatrix} \tilde{g}_{11}(s) & \tilde{g}_{12}(s) \\ 0 & \tilde{g}_{22}(s) \end{bmatrix} \quad (13)$$

where $\tilde{G}(s)$ is referred to inputs Δ_1 and Δ_2 . It is possible to arrive at a state-space representation such as the one given in (10)-(11) from the state representation (1) in two steps. First, the input transformation matrix E must result in BE^{-1} being diagonal. Since the matrix B can be written as:

$$B = \begin{bmatrix} -\frac{C_f}{mv_x} & 0 \\ 0 & \frac{C_f l_f}{I_{zz}} \end{bmatrix} \begin{bmatrix} 1 & \frac{C_r}{C_f} \\ 1 & -\frac{C_r l_r}{C_f l_f} \end{bmatrix} \quad (14)$$

then choosing E to be

$$E = \begin{bmatrix} 1 & \frac{C_r}{C_f} \\ 1 & -\frac{C_r l_r}{C_f l_f} \end{bmatrix} \quad (15)$$

results in \tilde{B} being diagonal:

$$\tilde{B} = BE^{-1} = \begin{bmatrix} -\frac{C_f}{mv_x} & 0 \\ 0 & \frac{C_f l_f}{I_{zz}} \end{bmatrix} \quad (16)$$

The resulting new inputs are given by:

$$\Delta_1 = \delta_f + \frac{C_r}{C_f}\delta_r, \quad \Delta_2 = \delta_f - \frac{C_r l_r}{C_f l_f}\delta_r \quad (17)$$

A physical interpretation of these new inputs is in terms of a mode Δ_1 where the front and rear wheels steer towards the same direction and in terms of a mode Δ_2 where the front and rear wheels steer in opposite directions. The equation of the yaw rate with respect to the inputs Δ_1 and Δ_2 is:

$$\frac{I_{zz}}{C_f l_f} \ddot{\psi} + \frac{C_f l_f^2 + C_r l_r^2}{C_f l_f v_x} \dot{\psi} = \Delta_2 + \left(1 - \frac{C_r l_r}{C_f l_f}\right) \beta \quad (18)$$

The second step consists of subtracting from the input Δ_2 the signal that results from applying a constant gain of value

$1 - \frac{C_r l_r}{C_f l_f}$ to the output β . The introduction of this cross-

feedback element results in a system with a state-space representation such as the one in (10)-(11). Thus, the 4-wheel steering control problem has been recast as the problem of controlling a 2 by 2 partially decoupled linear plant. The resulting control structure is depicted in Figure 4.

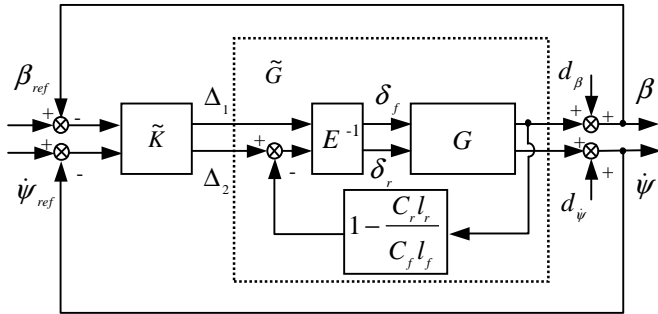


Figure 4. Proposed control scheme.

The matrix transfer function of the virtual plant \tilde{G} in Figure 4 is upper triangular.

5 Control design based on a linear model including tyre force dynamics and actuators

In this section, the control structure presented above is applied to the design of a diagonal controller \tilde{K} based on a more accurate linear model of the 4-wheel steering dynamics. This model, which is also based on the single-track simplification, incorporates tyre force dynamics and a second order model of the front and rear steering actuators. The dynamics of the tyre forces are modelled as:

$$\dot{S}_f = a(C_f \alpha_f - S_f), \quad \dot{S}_r = a(C_r \alpha_r - S_r) \quad (19)$$

where a is a speed-dependent parameter. The dynamics of the tyre forces and the models of the actuators have been incorporated into the state-space representation of the lateral dynamics of the single-track model. A 2 by 2 matrix transfer function $G(s)$ describing the steering response has been obtained from this new state-space representation. The control structure introduced in the previous section has been applied to design β and $\dot{\psi}$ controllers based on this $G(s)$.

The remainder of this section will present an example design of the controllers $\tilde{k}_1(s)$ and $\tilde{k}_2(s)$ for certain values of the parameters defining the car model and a longitudinal constant speed of $v_x = 14$ m/s.

5.1 Control specifications

The main requirements for the controlled 4-wheel steering car are:

- Tracking of sideslip and yaw rate reference signals with closed-loop bandwidth of 3 Hz (≈ 18 rad/s). These reference signals are obtained from the driver's steering-wheel input.
- Reject any disturbances in sideslip and yaw rate with the highest possible bandwidth (preferably with rise times of less than 300 ms, to avoid interference with the driver's reactions).
- Robustness with respect to reductions in the tyre stiffness of up to 30%.

The communication between the controllers and the steering actuators is subject to a time delay of 20 ms. This time delay induces an additional phase lag in the frequency response of the closed-loop system, thereby constraining the design by requiring larger phase margins.

5.2 Control design

A feature of the proposed control scheme is the possibility of using classical SISO loop-shaping techniques to design the two controllers individually, thereby simplifying the original multivariable design problem. Figure 5 shows the Bode plots of the transfer function $\tilde{G}(s)$ for a speed of $v_x = 14$ m/s.

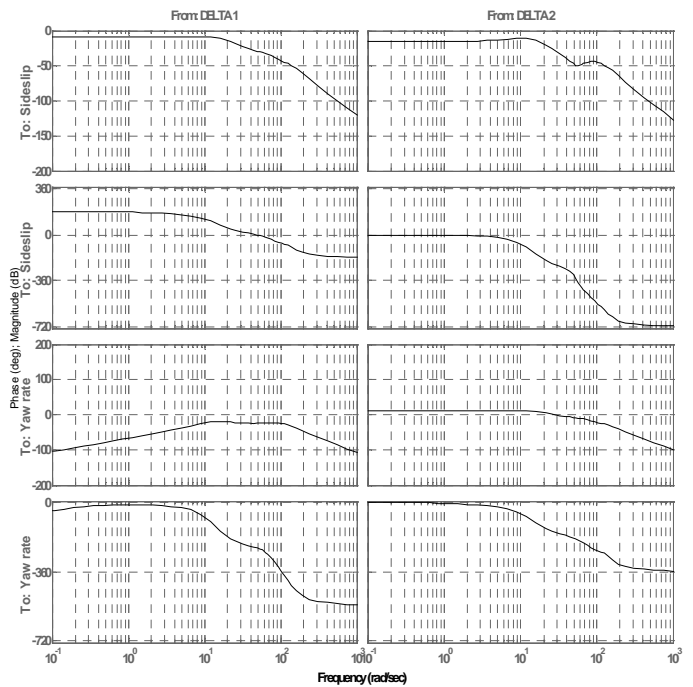


Figure 5. Bode plot of \tilde{G} with $v_x = 14$ m/s.

The Bode plot of the multivariable structure function $\tilde{\gamma}(s)$ is shown in Figure 6. As can be seen in Figures 5 and 6, $\tilde{G}(s)$ is not exactly upper-triangular. This is due to the effect of the tyre force dynamics and the actuators. However, it can be assumed that $\tilde{g}_{21}(s)$ and $\tilde{\gamma}(s)$ are small enough to be negligible at low frequencies. It is shown below that by relaxing the bandwidth requirements it is still possible to design $\tilde{k}_1(s)$ and $\tilde{k}_2(s)$ using SISO techniques.

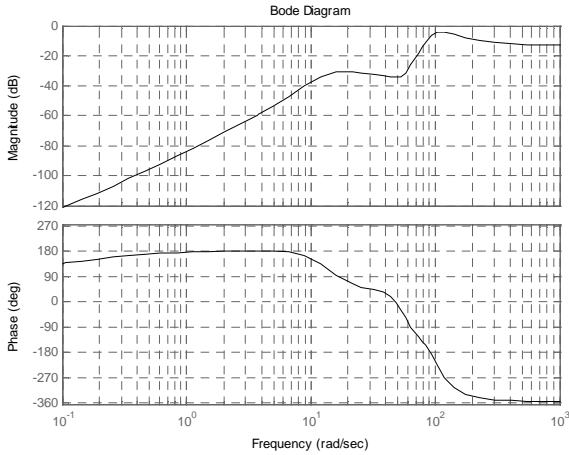


Figure 6. Bode plot of $\tilde{\gamma}$ for $v_x=14$ m/s.

If the sideslip channel is allowed to have a substantially lower bandwidth than the yaw rate channel, then the two controllers can still be designed on the basis of the corresponding $\tilde{g}_{ii}(j\omega)$ as two SISO systems using classical Bode plot-based loop shaping techniques. It is then assumed that the bandwidth of Channel 2 (yaw rate) is to be kept at approximately 18 rad/s and that the bandwidth of Channel 1 (sideslip) can be made substantially smaller. If that is the case, the influence of the term $\tilde{\gamma}(j\omega)\tilde{h}_2(j\omega)$ on the transmittance of Channel 1 can be neglected on the basis of the small magnitude of $\tilde{\gamma}(j\omega)$ at low frequencies and the channel's low bandwidth, as it can be assumed that \tilde{k}_1 causes the magnitude of $\tilde{k}_1(j\omega)\tilde{g}_{11}(j\omega)$ at higher frequencies to be small enough to make the influence of $\tilde{\gamma}(j\omega)\tilde{h}_2(j\omega)$ irrelevant. In addition, the influence of the term $\tilde{\gamma}(j\omega)\tilde{h}_1(j\omega)$ on the transmittance of Channel 2 can be neglected on the basis of the small magnitude of $\tilde{\gamma}(j\omega)$ at low frequencies and the roll-off of $\tilde{h}_1(j\omega)$ due to the lower bandwidth of Channel 1.

Figure 5 shows that the magnitude of $\tilde{g}_{21}(j\omega)$ rises to values around -20 dB for frequencies between 10 and 100 rad/s.

Consequently, the controller \tilde{k}_1 has to induce roll-off in $\tilde{h}_1(j\omega)$ so that the magnitude of $\frac{\tilde{g}_{21}(j\omega)\tilde{h}_1(j\omega)}{\tilde{g}_{11}(j\omega)}$ at those frequencies is such that adequate cross-coupling rejection for

Channel 2 is achieved. The fact that the bandwidth of Channel 1 has been chosen to be substantially smaller than that of Channel 2 provides for this requirement. On the other hand, the roll-off in $\tilde{g}_{12}(j\omega)$ for frequencies above 10 rad/s (see Figure 5) is regarded as sufficient to achieve satisfactory cross-coupling rejection in Channel 1. The peak in $\tilde{g}_{12}(j\omega)$ shown in Figure 4 is considered compensated by the roll-off in $\tilde{h}_2(j\omega)$ so that the magnitude of $\frac{\tilde{g}_{12}(j\omega)\tilde{h}_2(j\omega)}{\tilde{g}_{22}(j\omega)}$ is sufficiently low.

Considering the assumptions and remarks above, the design of the controllers \tilde{k}_1 and \tilde{k}_2 has been carried out on the basis of $\tilde{g}_{11}(j\omega)$ and $\tilde{g}_{22}(j\omega)$, respectively, using classical SISO Bode plot-based loop shaping. The following controllers have been designed:

$$\tilde{k}_1(s) = -10 \frac{\left(\left(\frac{s}{13} \right)^2 + 2 \cdot 0.50 \cdot \left(\frac{s}{13} \right) + 1 \right)}{s \left(\left(\frac{s}{15} \right)^2 + 2 \cdot 0.70 \cdot \left(\frac{s}{15} \right) + 1 \right)}, \quad (20)$$

$$\tilde{k}_2(s) = 3.8 \frac{\left(\left(\frac{s}{16} \right)^2 + 2 \cdot 0.50 \cdot \left(\frac{s}{16} \right) + 1 \right)}{s \left(\frac{s}{150} + 1 \right)}$$

These controllers result in phase and gain margins of over 70° and 16 dB for each of the channels. Figure 6 shows the Bode plots of the resulting closed-loop transfer functions.

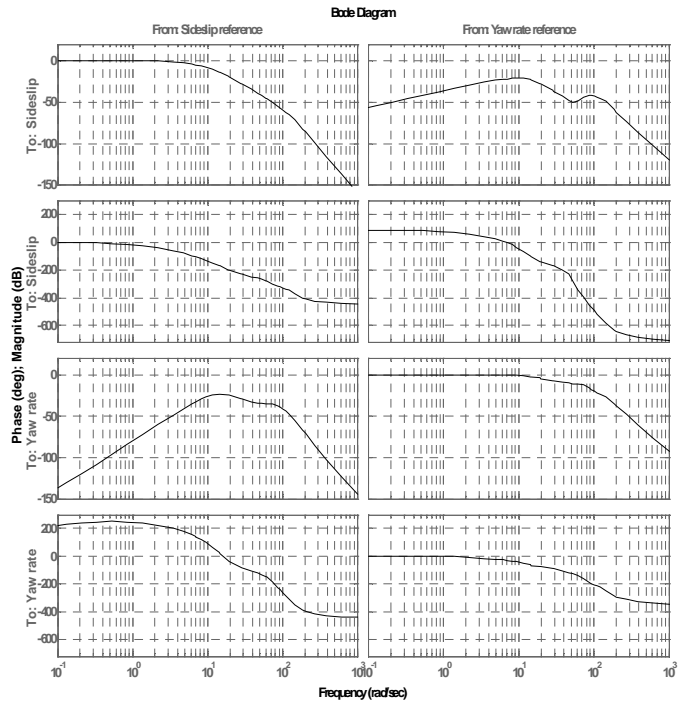


Figure 7. Bode plot of the closed-loop transfer functions.

6 Simulations

To illustrate the performance and robustness of the designed controllers, the response of the controlled car to a given control task has been simulated for different values of tyre cornering stiffness. The simulations have been carried out using the more accurate linear model used for design at a constant speed of 14 m/s. In the simulations, the 20 ms communication delay has been incorporated into the model of the actuators. The saturation limits and rate constraints of the actuators have also been included. The control task considered consists of tracking a yaw rate reference signal in the shape of a single rectangular pulse of 0.1 rad/s amplitude and 3 s width while maintaining zero sideslip.

Simultaneously, the steering control is required to reject any disturbances caused by a lateral gust of wind of 1 s duration. The effect of a lateral gust of wind on the car is considered equivalent to the effect of a force along the CM - y axis applied on the centre of mass, denoted as F_{yD} , together with a torque about the CM - z axis, denoted as M_{zD} . The effects of F_{yD} and M_{zD} on the car lateral dynamics have been included in the model used in the simulations. In the simulations presented here F_{yD} and M_{zD} are singular rectangular pulses of 1 s duration and magnitudes 1500 N and 1000 Nm, respectively. These values approximately correspond to a lateral gust of wind of 80 km/h. Figure 8 shows the result of simulating the effect of this gust of wind on the car at $v_x=14$ m/s assuming that neither the front nor and front wheel are steered.

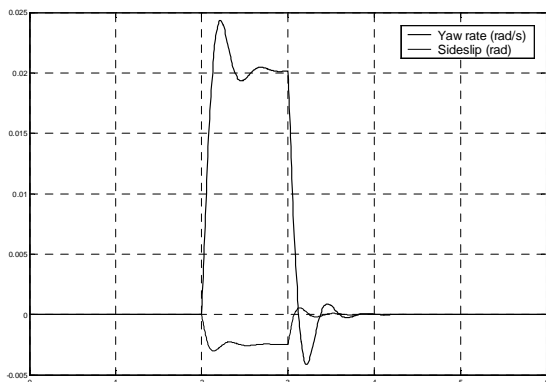


Figure 8. Effect of an 80 km/h gust of wind with no control

The response to the control task has been simulated with the nominal values of the cornering stiffness (Figure 9) and also with a 30% reduction in the cornering stiffness of the front and rear tyres (Figure 10). In the former case the steering control satisfactorily tracks the desired reference and rejects the disturbances. In the latter case the system remains stable though, as expected, the performance is worsened, particularly regarding the damping of the responses.

7 Conclusions and further research

The control structure proposed in this paper allows for the decomposition of the multivariable 4-wheel steering control design problem into two simpler SISO control design problems.

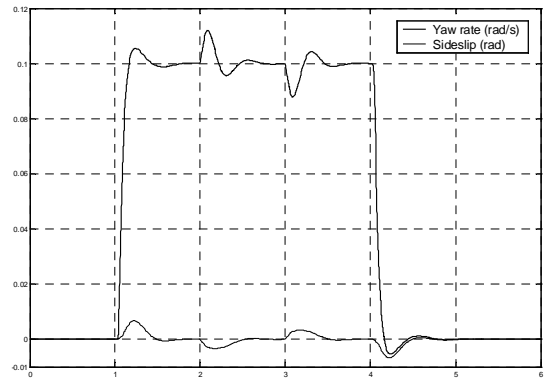


Figure 9. Response with nominal tyre stiffness

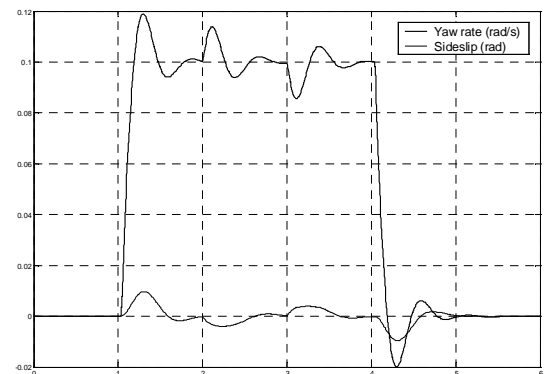


Figure 10. Response with 30% reduction in tyre stiffness

A design example implementing the proposed structure has been presented. In this example, the control design has been carried out using simple Bode plot-based loop shaping for each of the two channels. Bandwidth separation was imposed to preserve partial decoupling and to achieve satisfactory cross-disturbance rejection. The input transformation results in the steering control system distributing the control effort among the front and rear wheels.

Issues for further study are actuator saturation, robustness analysis and the use of gain scheduling to make the system operative over a certain range of speed.

8 References

- [1] Ackermann, J., Robust Decoupling, "Ideal Steering Dynamics and Yaw Stabilization of 4WS cars", *Automatica*, **Vol. 30**, No. 11, pp. 1761-1768, (1994).
- [2] Furukawa, Y., Yuhara, N., Sano, S., Takeda, H., Matsushita, Y., "A Review of Four-Wheel Steering Studies from the Viewpoint of Vehicle Dynamics and Control", *Vehicle System Dynamics*, **18**, pp. 151-186, (1989).
- [3] Gianone, L., Palkovics, L., Bokor, J., "Design of an active 4WS system with physical uncertainties", *Control Engineering Practice*, **Vol. 3**, No. 8, pp. 1075-1083, (1995).
- [4] O'Reilly, J., Leithead, W. E., "Multivariable design by 'individual channel design'", *International Journal of Control*, **Vol. 54**, No. 1, pp. 1-46, (1991).